Chapter 1

A Level-Set method for three dimensional bifluid flows evolving in square micro channels

C-H. Bruneau, T. Colin

IMB University of Bordeaux 1, MC2 INRIA Bordeaux Sud Ouest, 351 Cours de la Libération, 33405 Talence, France
bruneau@math.u-bordeaux1.fr, colin@math.u-bordeaux1.fr

S. Tancogne*

University of Reims Champagne-Ardenne, UFR Sciences exactes et naturelles, Moulin de la Housse, BP 1039, 51687 Reims Cedex 2, France
sandra.tancogne@univ-reims.fr

In this paper, a numerical method in order to study the fluid dynamics of diphasic flows evolving in micro channels is presented. These flows are characterized by the predominance of the interfacial phenomenons because of the surface tension effects. Technically, the Stokes equations are solved for the hydrodynamic part and the interface is moved thanks to the Level Set method introduced by Osher and Sethian. The results are compared with experimental data and the three dimensional effects are commented. In addition, the numerical techniques employed are emphasized.

1.1. Introduction

Microfluidics deal with the manipulation and the control of liquids in channels about a hundred of microns in the cross flows directions[14] . The typical velocity of such flows is about one centimeter per second. As a consequence, the Reynolds number is small, the flows are laminar and the motion of the interface between the two fluids is controlled by the effect of the surface tension. Since there are no turbulent effects, the experimental researcher developed experimental tools to mix the flows and to control their evolution. Two different configurations are considered in this paper. The first one is composed by two coaxial cylinders of circular and square sections. Since the two flows are non miscible and Newtonian, this leads to several regimes of flows: jets and droplets[9] . The use of coflows or drippings find his interest in various industrial[8] and biological applications[19] like ink jet printing or spray atomization for example. It is then necessary to control the evolution of the diphasic flow in order

*Corresponding author.

to produce droplets of different shape and volume. The created micro droplets are often employed for their internal dynamics to mix products that are generally toxic and expensive. The second configuration corresponds to square micro channels with a T-junction. The use of such capillaries allows to control the evolution of the micro droplets and to optimize the mixing of the substances inside the micro droplets by changing their shape. In addition, it is possible to measure the shear rates of the flows. In a T-junction, the flows are parallel. If the flow rates, the position of the interface between both flows and the viscosity of one fluid are known, it is possible to deduce the viscosity of the other fluid. Such a configuration is named a rheometer[8] . In this context, the numerical difficulties are due to the fact that it is necessary to follow the interface between two flows knowing that the three dimensional effects must be put forward. It is well-known that the breaking jet phenomenon, due to the Plateau-Rayleigh instability, is only observable thanks to a three dimensional modeling. The numerical simulation of two phases is nowadays a topic research largely investigated. The main challenge is to follow a moving interface between two fluids, knowing that it will undergo significant changes. There exist many interface tracking methods, classically divided into two main categories: the Lagrangian and the Eulerian methods. It is possible to quote among them, the front tracking method, the moving grid method, the Volume-Of-Fluid method and the Level Set method. Each of these methods have drawbacks and advantages. In this study, it is important that the method takes into account the topological changes and allow a precise calculation of the curvature at the front. The moving grid method takes into account the jump conditions at the interface and it is possible to combine it with high order schemes. But its use is limited to flows that do not show large strains. The Front Tracking method solves well the interface problem, but a poor distribution of particles yields a loss of accuracy. Moreover, the topological changes require a redistribution of the particles that makes difficult the extension to the three dimensional case. The literature shows that the VOF methods, introduces by DeBar in 1974[4] , are largely used and give interesting results[18] . However, these methods present a main drawback as the interface is diffuse, besides its implementation is costly in three dimensional configurations. The Level Set method introduces by Osher and Sethian[15,16] has many advantages, the first of all is the ease to extend it to the three dimensional case. Besides, the geometric property of the Level Set function allows to compute precisely algebraic terms like the normal vector and the curvature at the interface. When this method is coupled with a careful computation of the distance of the mesh points[20] , the topological changes are well managed.

This paper is organized as follows. The second section is dedicated to the presentation of the governing equations. The Stokes equations with interface and the level Set method are presented. Discretizations and schemes employed are the subject of the third part. At this stage, is discussed the required stability condition when capillary effects are considered. The fourth part is devoted to the presentation of the numerical results. Finally, the numerical aspects linked to the development of

a three dimensional tool for complex geometries with a specific boundary condition between the wall of the micro channel and the inside flows are detailed.

1.2. Modelling

1.2.1. *The Stokes equations for diphasic flows in microfluidic*

We consider the Navier-Stokes equation for each Newtonian flow

$$\rho\left(\frac{\partial U}{\partial t}+(U.\nabla)U\right)=\rho f-\nabla P+\nabla.[\eta\nabla U] \tag{1.1}$$

where U is the velocity of the flow, ρ the density, η the viscosity, P the pressure and f denotes the external forces like the gravity and the interface condition

$$[\sigma(U,P)\mathbf{n}]=\gamma\kappa\mathbf{n} \tag{1.2}$$

where γ is the surface tension, $\mathbf{n}$ the unit normal vector pointing outside of the considered flow to the interface and κ the average curvature.

The characteristic dimensions L and V associated respectively to the length of the micro channel and the main velocity are introduced. With this notations, we consider the classical dimensionless numbers: $\mathcal{R}e$ the Reynolds number, $\mathcal{C}a$ the capillary number and $\mathcal{B}o$ the Bond number defined by

$$\mathcal{R}e=\frac{\rho VL}{\eta},\ \mathcal{C}a=\frac{\eta V}{\gamma}\ \text{ and }\ \mathcal{B}o=\frac{\rho gL}{\gamma}.$$

For the microfluidic geometries considered, the sections of the capillary are about a hundred of micrometers and the flows velocities are around a centimeter per second. The Reynolds number is generally fewer than one hundred, the capillary number is contained between 10^{-6} and 10^{-2} and the Bond number between 10^{-9} and 10^{-1}. These low Reynolds numbers make the inertial effects small in front of the viscous ones. In this paper, we consider only flows where the Reynolds number is close to one so that the unsteady term is negligible. In addition, the gravitational effects are also negligible. Thus, with these hypothesis, the Navier-Stokes equations reduce to the linear Stokes equations. Moreover, the value of the capillary number induces that the surface tension effect dominates the viscous one meaning that the interface phenomenon is driven by the capillary effects. Thanks to the previous considerations, we consider now the Stokes equations for two fluids in a bounded domain $\Omega\subset\mathcal{R}^3$. The two fluids, respectively called internal (i) and external (e), occupy respectively at each time t the domains $\Omega_i(t)$ and $\Omega_e(t)$ such that $\Omega=\Omega_i(t)\cup\Omega_e(t)\cup\Gamma(t)$. The interface $\Gamma(t)$ between the two fluids is defined by $\Gamma(t)=\bar{\Omega}_i(t)\cap\bar{\Omega}_e(t)$.

So, the hydrodynamic model is the following

$$\begin{cases} div(2\eta D(U))=\nabla P+\gamma\kappa\delta_\Gamma\mathbf{n}_\Gamma \text{ in } \Omega \\ \nabla.U=0 \text{ in } \Omega \end{cases} \tag{1.3}$$

where $D(U)$ is the deformation rate tensor given by $D(U) = \frac{\nabla U + (\nabla U)^T}{2}$, η is the dynamic viscosity such that

$$\eta = \begin{cases} \eta_i & \text{in the internal flow} \\ \eta_e & \text{in the external flow} \end{cases} \tag{1.4}$$

and $\gamma\kappa\delta_\Gamma \mathbf{n}_\Gamma$ denotes the surface tension contribution at the interface with δ_Γ the Dirac mass on Γ

$$\forall h \in C_0^0(\Omega), \ < \delta_\Gamma, h >= \int_\Gamma h(x) d\sigma \tag{1.5}$$

and $\mathbf{n}_\Gamma$ is the unit vector normal to the interface Γ.

1.2.2. *The boundary conditions*

The Stokes equations are associated to boundary conditions. At the entrance section of the micro channel, the velocity profile is imposed

$$U.n_{\Gamma_1} = u_{inj} \tag{1.6}$$

where n_{Γ_1} is the unit normal vector. The details concerning the computation of the velocity u_{inj} are given in the section devoted to the numerical results.

At the solid wall, the imposed condition is a Robin condition

$$\begin{cases} U.\tau = \alpha(\eta) \frac{\partial U.\tau}{\partial n}, \\ U.n = \quad 0, \end{cases} \tag{1.7}$$

with $\alpha(\eta)$ an experimental data and τ the tangent vector. This condition allows the fluid to slip on the wall.

The output condition is more difficult to define because in some cases two fluids come out of the canal. Drawing on the work of Bruneau[2,3] , an alternative solution was to calculate for each time step the velocity profile. Knowing the position of the interface a few cells before the exit section, the resolution of a 2D Stokes equation (like at the entrance condition) gives us a velocity profile to impose.

1.2.3. *The Level Set method: parameterization of the interface*

Our objective is to follow the evolution in the time interval $(0, T)$ of the interface between the two fluids. In our work, the interface is represented thanks to the level function $\phi(t, x, y, z)$[21] . At the initial time, ϕ is zero at the interface, negative in one phase and positive in the other

$$\phi(0, x, y, z) = \begin{cases} < 0 \text{ in flow i}, \\ > 0 \text{ in flow e}, \\ 0 \quad \text{at the interface } \Gamma. \end{cases} \tag{1.8}$$

Its motion is governed by an advection equation

$$\begin{cases} \partial_t \phi + (U.\nabla)\, \phi = 0 & \text{in } \Omega \times (0, T), \\ \phi(t = 0) = \phi(0, x, y, z) & \text{in } \Omega. \end{cases} \tag{1.9}$$

Such a modelling implies the properties of the Level Set function to be respected at each time step. In particular, the fact that the interface is represented by the zero value of the function ϕ

$$\forall t \geq 0, \quad \Gamma(t) \; = \; \{(x, y, z), \; \phi(t, x, y, z) = 0\} \, . \tag{1.10}$$

When ϕ is known, the unit normal $\mathbf{n}_\Gamma$ at the interface and the curvature κ are computed as follow

$$\mathbf{n}_\Gamma = \left. \frac{\nabla \phi}{|\nabla \phi|} \right|_{\phi=0} \text{ and } \kappa = \nabla . \left(\left. \frac{\nabla \phi}{|\nabla \phi|} \right) \right|_{\phi=0} . \tag{1.11}$$

1.3. The numerical method

Now, we proceed to the discretization of the equations introduced in the previous section. For the presentation of the whole algorithm, we refer the reader to[22] .

1.3.1. *The advection equation*

The time discretization of the advection equation (1.9) is explicit and a classical Euler scheme is used

$$\phi^{n+1} = \phi^n - \Delta t (U^n . \nabla) \phi^n \tag{1.12}$$

where Δt is the time step and $n + 1$ denotes the new iteration at time $t^{n+1} = (n + 1)\Delta t$. This choice is associated to a restriction on the time step (the classical CFL condition) in order to ensure the stability and so the convergence.

The space discretization is made with a five order WENO scheme[12] . The WENO schemes are based on the ENO ones introduced by Harten et al. in 1987. The main idea is to use the more regular stencil between several one in order to approximate the flux at the edge of two cells. The aim is to increase the accuracy and to prevent the oscillations around the shocks.

The different steps of the construction of the scheme are now recalled. For the sake of simplicity, the one dimensional case is presented below. First of all, the

following coefficients are computed

$$v_1^- = \frac{\phi_{i-2,j,k} - \phi_{i-3,j,k}}{\Delta x}, \quad v_1^+ = \frac{\phi_{i+3,j,k} - \phi_{i+2,j,k}}{\Delta x}$$

$$v_2^- = \frac{\phi_{i-1,j,k} - \phi_{i-2,j,k}}{\Delta x}, \quad v_2^+ - = \frac{\phi_{i+2,j,k} - \phi_{i+1,j,k}}{\Delta x}$$

$$v_3^- = \frac{\phi_{i,j,k} - \phi_{i-1,j,k}}{\Delta x}, \qquad v_3^+ = \frac{\phi_{i+1,j,k} - \phi_{i,j,k}}{\Delta x}$$

$$v_4^- = \frac{\phi_{i+1,j,k} - \phi_{i,j,k}}{\Delta x}, \qquad v_4^+ = \frac{\phi_{i,j,k} - \phi_{i-1,j,k}}{\Delta x}$$

$$v_5^- = \frac{\phi_{i+2,j,k} - \phi_{i+1,j,k}}{\Delta x}, \quad v_5^+ = \frac{\phi_{i-1,j,k} - \phi_{i-2,j,k}}{\Delta x}$$

where the exponents + and - are associated to the derivatives $\frac{\partial \phi^-}{\partial x}$ et $\frac{\partial \phi^+}{\partial x}$. In the three dimensional case, the formula are the same in the other directions. Then, the expression of the derivative $\frac{\partial \phi}{\partial x}$ is obtained by

$$\frac{\partial \phi}{\partial x} = w_1 \left(\frac{v_1}{3} - \frac{7v_2}{6} + \frac{11v_3}{6} \right) + w_2 \left(-\frac{v_2}{6} + \frac{5v_3}{6} + \frac{v_4}{3} \right) + w_3 \left(\frac{v_3}{3} + \frac{5v_4}{6} - \frac{v_5}{6} \right) \tag{1.13}$$

where the weight are

$$w_1 = \frac{a_1}{a_1 + a_2 + a_3} \, , w_2 \frac{a_2}{a_1 + a_2 + a_3} \, , w_3 = \frac{a_3}{a_1 + a_2 + a_3}$$

with

$$a_1 = \frac{1}{10} \frac{1}{(\epsilon + S_1)^2} \, , a_2 = \frac{6}{10} \frac{1}{(\epsilon + S_2)^2} \, , a_3 = \frac{3}{10} \frac{1}{(\epsilon + S_3)^2},$$

$$\epsilon = 10^{-6} max(v_1^2, v_2^2, v_3^2, v_4^2, v_5^2) + 10^{-15},$$

and

$$S_1 = \frac{13}{12}(v_1 - 2v_2 + v_3)^2 + \frac{1}{4}(v_1 - 4v_2 + 3v_3)^2,$$

$$S_2 = \frac{13}{12}(v_2 - 2v_3 + v_4)^2 + \frac{1}{4}(v_2 - v_4)^2,$$

$$S_3 = \frac{13}{12}(v_3 - 2v_4 + v_5)^2 + \frac{1}{4}(3v_3 - 4v_4 + v_5)^2.$$

To conclude, the derivative is computed like in the case of the upwind scheme according to the direction of propagation.

$$\begin{cases} \dfrac{\partial \phi}{\partial x} = \dfrac{\partial \phi^+}{\partial x} \; if \; u_{i,j,k} < 0, \\ \dfrac{\partial \phi}{\partial x} = \dfrac{\partial \phi^-}{\partial x} \; if \; u_{i,j,k} > 0. \end{cases} \tag{1.14}$$

The implementation of the WENO scheme requires the knowledge of the values of $\phi_{i,j,k}$ out of the domain Ω. These valuess will be evaluated thanks to linear extrapolations of the known values inside Ω.

1.3.2. *The hydrodynamic part*

The discretization of the incompressible Stokes equations is classical. The finite volume method on structured staggered grids is considered (Patankar, 1980). The idea is to associate different control volumes grids to the different unknowns[5] . Each unknown is located at the center of the control volumes of the associated meshes. In our Cartesian three-dimensional case, the cells consist in cubes. A typical grid is composed by a main grid associated to the pressure and three secondary grids associated to the three components of the velocity. The mesh associated to the first component of the velocity is represented on Fig.1.1 . The three Stokes equations are

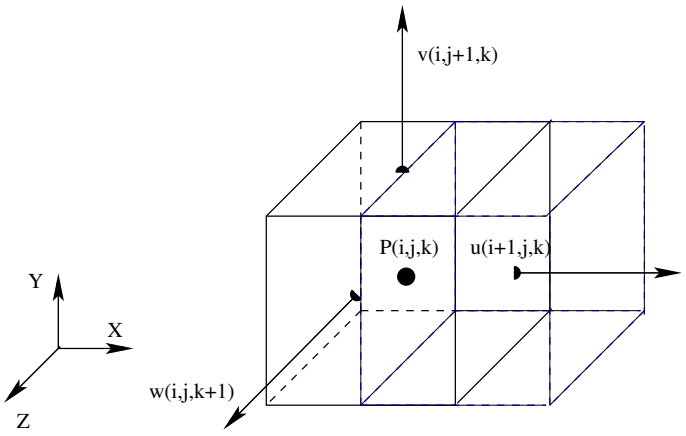

Fig. 1.1. MAC mesh cell (solid line) with a control volume (dashed line) of the first component of the velocity vector $u(i+1,j,k)$.

associated to a component of the velocity and thus integrated over the considered control volumes. The continuity equation is integrated over the control volumes of the pressure (the original mesh). Although, the Stokes equations are steady, the time discretization of the capillary unknowns is explicit and so the following scheme is used

$$\begin{aligned} \nabla.(2\eta^n D(U^{n+1})) &= \nabla P^{n+1} + \gamma\kappa^n\delta(\phi^n)\nabla\phi^n, \\ \nabla.U^{n+1} &= 0. \end{aligned} \tag{1.15}$$

This explicit choice introduces an usual CFL condition on the time step. This point is the subject of the next subsection. To compute (U^{n+1}, P^{n+1}), the Augmented Lagrangian method[6] is used. This algorithm presents numerous advantages:

the ease of the implementation, the reduction of the size of the linear system and an improvement of the shape of the matrix. The whole algorithm is the following:

(1) **Initial data**
At t^n the known variables are U^n, P^n, η^n and ϕ^n.

(2) **Computation of U^{n+1} and P^{n+1}**
(a) We assume $V_U^0 = U^n$ and $V_P^0 = P^n$ and V_U^k, V_P^k denote the intermediate variables the Lagrangian step k.
(b) Then, we solve the following linear system until the convergence criterion is achieved.

$$\begin{aligned} \nabla.\left(2\eta^n D(V_U^{k+1})\right) + r\nabla\left(\nabla.V_U^{k+1}\right) &= \nabla V_P^k + \gamma\kappa^n\delta(\phi^n)\nabla\phi^n, \\ V_P^{k+1} &= V_P^k - s(\nabla.V_U^{k+1}), \end{aligned} \tag{1.16}$$

with r and s two fixed parameters that are fixed here to 1 ($r = s = 1$).
(c) When the criterion $\nabla.V_U^{k+1} < \epsilon$ (with $\epsilon \approx 1.e^{-04}$) is achieved, we set

$$U^{n+1} = V_U^{k+1},\ P^{n+1} = V_P^{k+1}.$$

(3) **Computation of ϕ^{n+1}**
The Level Set function is moved

$$\phi^{n+1} = \phi^n - \Delta t U^{n+1}(\nabla\phi^n).$$

(4) **Updating of the viscosity η**

$$\eta^{n+1} = \eta_1 + (\eta_2 - \eta_1)H(\phi^{n+1}),$$

with the Heaviside distribution H defined as

$$H(x) = \begin{cases} 1 & \text{if } x > 0, \\ 0 & \text{if } x \leq 0. \end{cases} \tag{1.17}$$

1.3.3. *A restrictive stability condition*

In the Stokes equations, the explicit treatment of the term associated to the surface tension required a stability criterion to maintain the convergence of the method. Commonly, the criterion proposed by Brackbill, Kote and Zemach is used[1]

$$\Delta t = \sqrt{\frac{1/2(\rho_1 + \rho_2)(\Delta x)^3}{2\pi\gamma}}, \tag{1.18}$$

where ρ_1, ρ_2 are the densities of the fluids. However, it turns out that for the microfluidic applications, this condition becomes very restrictive. Indeed, the space step is generally about 10^{-6} m. As a consequence, the time step takes values close to 10^{-8}s.

The derivation of the Brackbill condition is based on the study of the contribution of the unsteady and inertial terms. The contribution of the densities of the two fluids in the condition (1.18) is a consequence of the analysis. Recently, a less restrictive stability condition was proposed by Galusinski and Vigneaux[7]

$$\Delta t_\gamma \leq c_2 \frac{min(\eta_1, \eta_2)}{\gamma} \Delta x \tag{1.19}$$

where c_2 is a constant that does not depend on the discrete parameters. This new condition takes into account the characteristics of the microfluidics flows. Indeed, the flows belong to the low Reynolds numbers hydrodynamics and the shape of the interface is generally quickly obtained. The derivation of the new condition is based on the estimation of the velocity induced by a small perturbation of the interface. If the displacement of the interface is high, the perturbation will be increased and will oscillate around the interface. The condition (1.19) assumes that if the displacement of the interface is lower than the amplitude of the perturbation then the oscillations are deleted. Finally, in the numerical computations, the time step Δt is chosen as the minimum value between the value given by the classical CFL condition and those given by the above condition due to the explicit treatment of the surface tension term

$$\Delta t = min(\Delta t_{cfl}, \Delta t_\gamma). \tag{1.20}$$

1.4. Numerical results in a square micro channel

1.4.1. *Experimental considerations*

The numerical simulations proposed are based on the following experimental configuration[9] . The jet is generated with a cylindrical capillary centred in a square capillary as shown in the Fig.1.2.

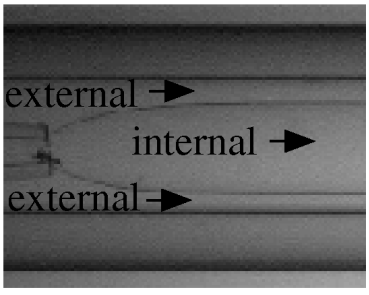

Fig. 1.2. Experimental configuration: cutting of a representative configuration of two non miscible flows named internal and external.

The external flow is injected by the external micro channel and the internal flow by the internal one. In this configuration, several kinds of micro droplets can be observed varying the internal or the external flow rate of the fluids. The numerical configuration reproduces the experimental setup.
The two flows are supposed to be injected separately. In a three dimensional configuration, the profile for the internal flow is analytically known since it is of parabolic type in a cylindrical channel (a classical Poiseuille flow). However, the external profile is a little more complicated. First, the corresponding domain is defined on the Cartesian mesh by penalising the injector in the square section, the more the meshing is fine, the more the representation of the injector is precise. Then, we have to compute the velocity profile solving the discrete simplified Stokes equations since the flow is supposed to be unidirectional[11] .

A typical profile employed to simulate the injection of the two flows is proposed in Fig.1.3 . The internal and external flows rates take the following values: $Q_e = 4500\mu L/h$ and $Q_i = 2500\mu L/h$, the external micro channel has a square section $S_c = 500\ \mu m$ and the radius of the cylindrical tube is $R_i = 100\ \mu m$. The outlet

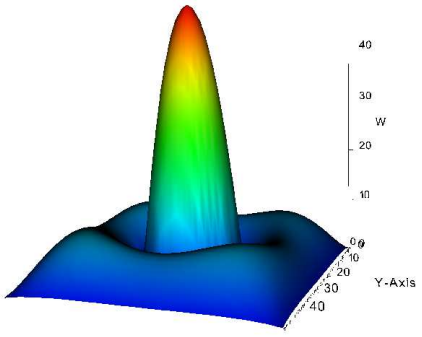

Fig. 1.3. Typical profile employed to simulate the experimental configuration of coaxial cylinders.

condition is obtained with a similar method than the one proposed in[2] and[3] . It consists to use at each time step the solution obtained at the previous time step.

Numerically, the consideration of such an injection condition requires a special treatment. The Fig.1.4 presents the first steps of the numerical computation. The representation of the injection needs to fix the velocity of the flow on several meshes. As it is shown on Fig.1.4, the evolution of the injection condition creates a singularity on the profile of the Level Set function at the interface (solid line). The presence of this singularity is fatal during the resolution of Stokes equations since the Level Set function is used to evaluate the curvature at the interface. To overcome this

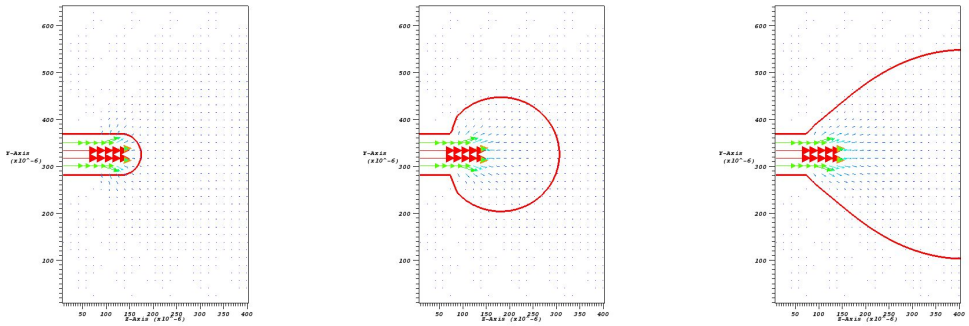

Fig. 1.4. From left to right: evolution of the injection in a square capillary of two fluids initially separated by a circular one .

difficulty, the hydrodynamic part is not solved on the all domain but only where the Level Set function is smooth as shown in Fig.1.5.

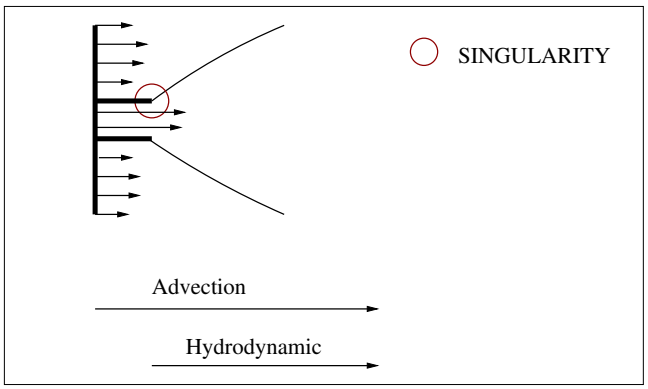

Fig. 1.5. Numerical representation of the injector.

1.4.2. *Jets, droplets and plugs*

The break-up of one fluid into another one is a complex phenomenon due to the Rayleigh-Plateau instability[17] . This instability is an hydrodynamic instability linked to the surface tension effects. So, to minimize its exposed surface a cylinder of liquid at rest will naturally break to create cheaper energy droplets. This phenomenon is of course only observable in three dimensions[10] . Let us focus on the numerical results. Here, the external micro channel has a square section $S_c = 550\ \mu m$ and the radius of the cylindrical tube is $R_i = 105\ \mu m$. The inner fluid

has a viscosity $\eta_i = 55mPa.s$ and the outer one $\eta_e = 235mPa.s$. The surface tension between the two fluids is $\gamma = 24mN/m$. In Fig.1.6, three sets of flow rates are considered: ($Q_i = 7500\mu L/h$, $Q_e = 6000\mu L/h$), ($Q_i = 2500\mu L/h$, $Q_e = 3000\mu L/h$) and ($Q_i = 2500\mu L/h$, $Q_e = 5500\mu L/h$). According to these flow rates, different regimes are observed as in the experiments.

The first set corresponds to the case of an oscillating jet: the internal fluid oscillates in the external one by is not pinched. Then, the second regime leads to the formation of a succession of droplets with the same shape and that are periodically created. Finally, a confined droplet, named a plug, is observed for the third set.

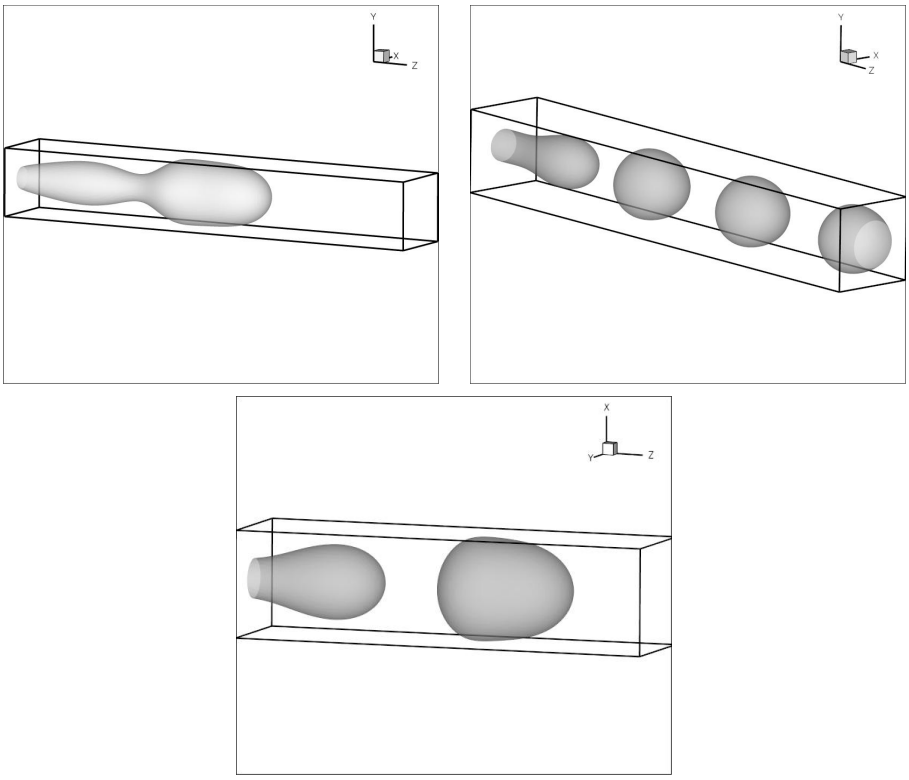

Fig. 1.6. From left to right: an oscillating jet, a succession of droplets and a plug (the internal flow alone is represented).

In microfluidic experiments, the droplets are confined and the surface tension drives their shape. These droplets are used as micro reactors or micro mixers. To understand their internal dynamics, it is interesting to know the droplets velocity field in their own referential. To do so, it is necessary to calculate the speed of the drop in its own frame of reference. When a droplet moves in a straight micro

channel, it stabilises so that his movement is associated with a known speed of translation. So the total velocity of the flow can be written as the sum of the translation velocity and the velocity of the droplet in its frame of reference. In other word, we write

$$U = U_T + V \tag{1.21}$$

where the translation velocity U_T is a parallel vector to the wall of the capillary and V is the velocity of the droplet. For more details, we refer the reader to[7] . The shape of the previous plug is plotted on Fig.1.7. It shows the effects due to the square section of the external capillary. In the plane (x,y), the shape of the plug is not anymore circular Fig.1.7 on the right and the external flow circulates only by the corners of the square micro channel.

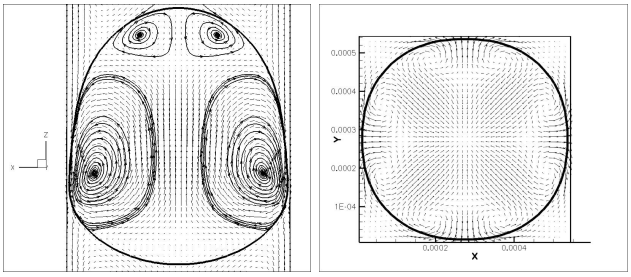

Fig. 1.7. Example of the use of droplets as micro mixers (shape of the droplets in different slices, velocity field in the droplet frame of reference and few streamlines). Left: shape and velocity field in the plane(x,z); right: view of the plug in the plane(x,y).

1.4.3. *Discussions*

In[22] , using an approach based on the linear theory of stability, a stability criterion is proposed. Thanks to this one, the flow regime (jet or droplets) can be predicted knowing the dimension of the external capillary, the flow rates and the properties of the two fluids. In addition, the stability length corresponding to the length of the jet just before the creation of the micro droplet can be computed. However, the study is based on the knowledge of the steady state and the perturbation of this one. In order to be as realistic as possible, it could be necessary to take into account the radius of the internal injector. In Fig.1.8, three representations of the flow are plotted. The properties of the two fluids are defined in subsection 1.4.2. The external capillary is about $650\mu m$ of section and the diameter of the injector is respectively $60\mu m$, $120\mu m$ and $273\mu m$ with the same flow rate. These numerical results show that there exists a stability area since the stability length is approximately the same in each case. Generally, for this kind of configuration, the jet tends towards the steady state solution before breaking-up. It is clear that the

diameter of the stable jet is about the same whatever the diameter of the injector is. Here, as the diameter of the stable jet is around $180\mu m$, the diameter of the flow increases or decreases according to the diameter of the injector to reach this value. Then, the jet breaks to give rise to droplets of diameters twice as large as its own diameter. On Fig.1.8, the droplets are plotted at the same position but do not correspond to the same time of simulation. Indeed, the flow rate being constant, the velocity of the jet is very different and so are the time of formation of the droplets and the distance between them. The higher the velocity is, the shorter the distance is.

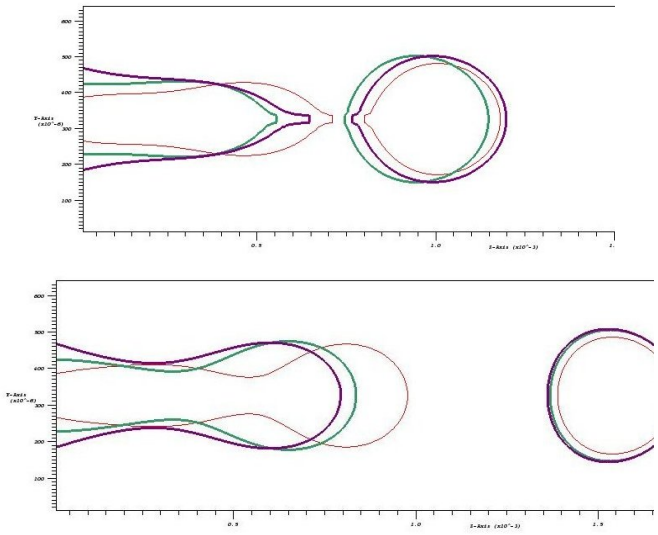

Fig. 1.8. Relation between the section of the injector and the volume of the created droplet: representation of the three different configurations at the same position.

1.5. The particular case of a T-junction

1.5.1. *The physical constraints and the numerical point of view*

The computation of fluids dynamics in micro channels with junctions is required to simulate the variety of experimental configurations. However, this task turns out delicate in the three dimensional case for two reasons. The first difficulty is due to the fact that a finite volume method on structured grid is employed and the second is induced by the different boundary conditions (Neumann, Dirichlet, Robin..) used.

If the simulations are made in a simple capillary, the implementation is quite easy when we choose to solve the linear system with an iterative procedure. Indeed, the

domain of computation can be meshed quickly with a local numbering (at a position (i, j, k) the neighbours are known automatically) and the boundary conditions are taken into account just by adding a layer of cells. In the case of the capillaries with junctions, the cells have to be numbered globally. Indeed, it is difficult to work with a local numbering since the various boundary conditions requires a lot of particular cases.

To handle the global numbering an *identity card* is associated to each cell of the mesh as follows:

```
type mesh
logical                    ::  wall
integer                    ::  FNDBC, FHDBC
integer                    ::  FNBC
integer                    ::  indcl
integer                    ::  ip, in, jp, jn, kp, kn
integer, dimension(1:3)    ::  indvar
end type mesh
```

The key words have the following meaning:

- **wall** localizes the cell in the geometry (true if the cell is on the wall, false otherwise)
- The three variables **FNDBC** (face with non homogeneous Dirichlet boundary condition), **FHDBC** (face with homogeneous Dirichlet boundary condition) and **FNBC** (face with homogeneous Neumann boundary condition) stand to identify the kind of boundary conditions on a face of the cell. These variables take for example the value 0 for none, 2^i if face i is concerned or $2^i + 2^j$ if faces i and j are concerned.
- **indcl** gives the number of the face of the cell that is on the wall. This variable is required to detect the faces of the cell that are on the boundary.
- **ip, in, jp, jn, kp, kp** give the increment to access to the neighbours
- **indvar** numbers the components (u, v, w) of the velocity U.

The following pictures illustrate the principle of identification of the cells. To achieve this goal, we remember the discretize variables (with local numbering, Fig.1.9) and we consider a very simple case, a T-junction composed by four cells (with global numbering). On the Fig.1.10, the fluids enter through the first and third cells and exits by the fourth one. A fictitious layer of cells is also required but it is not represented on Fig.1.10.

In this case, the declaration of the variables writes in Fortran 90

$$\mathbf{type(mesh)}, \mathbf{dimension}(:) :: \mathbf{c}$$

and the variable c takes the following values:

```
c(1:4)%wall=    True
```

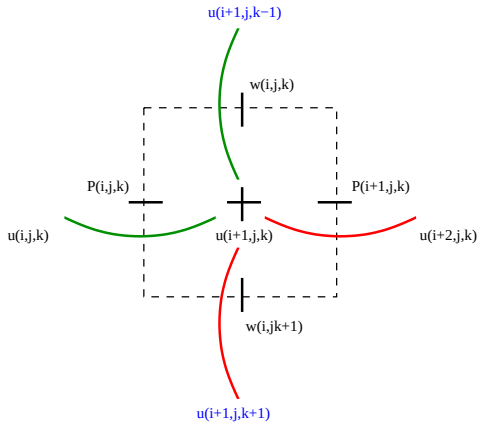

Fig. 1.9. Representation of the variables involved for the computation of $u(i+1,j,k)$ with the first equation of momentum.

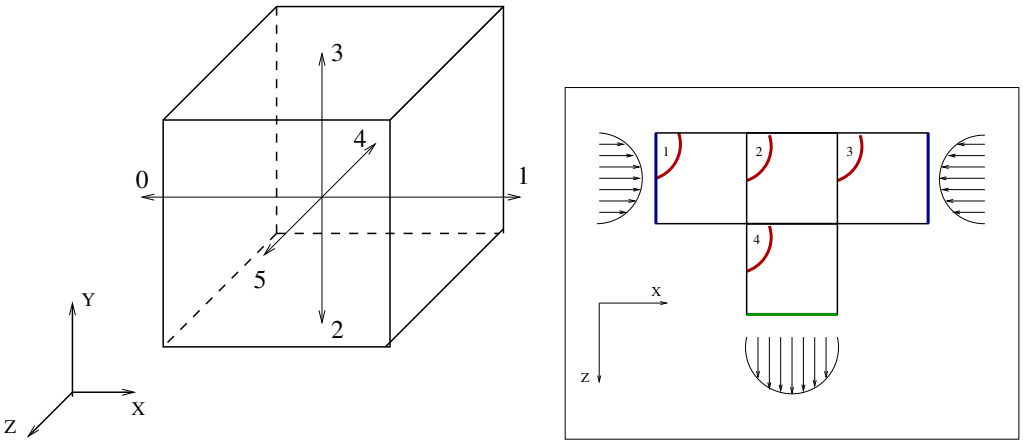

Fig. 1.10. Representation of a 3D cell (left) and of the four cells T-junction in the plane (x,z) (right).

$$\left|\begin{array}{ll|ll} \text{c(1)\%FNDBC} & =2^0 & \text{c(1)\%FHDBC} & =2^2+2^3+2^4+2^5 \\ \text{c(2)\%FNDBC} & =0 & \text{c(2)\%FHDBC} & =2^2+2^3+2^4 \\ \text{c(3)\%FNDBC} & =2^1 & \text{c(3)\%FHDBC} & =2^2+2^3+2^4+2^5 \\ \text{c(4)\%FNDBC} & =0 & \text{c(4)\%FHDBC} & =2^0+2^1+2^2+2^3 \end{array}\right|$$

c(1)%FCN	=0	c(1)%indcl	$=2^0+2^2+2^3+2^4+2^5$
c(2)%FCN	=0	c(2)%indcl	$=2^2+2^3+2^4+2^5$
c(3)%FCN	=0	c(3)%indcl	$=2^1+2^2+2^3+2^4+2^5$
c(4)%FCN	$=2^5$	c(4)%indcl	$=2^0+2^1+2^2+2^3+2^5$

```
for i=1:4
c(i)%indvar(1)   =   3*(i-1)+1
c(i)%indvar(2)   =   3*(i-1)+2
c(i)%indvar(3)   =   3*(i-1)+3
```

and we make up the numbering of the fictitious domain by a classical incrementation.

Once these informations are set, Stokes equations are solved for each component of the velocity integrating them on the associated control volume. Then we get a sparse matrix containing the coefficients given by the Stokes equations in which the boundary conditions are specified. The advantage of this approach is that equations and boundary conditions are written in a generic way. Taking them into account depends on the data contained in the variable of type "mesh". The exploitation of such data is then made through the "Btest" function of the Fortran 90 language.

1.5.2. *Coalescence of droplets in a T-junction*

The analysis of the break-up of a diphasic jet shows that the Level Set method manages well the topological changes. The study of the micro droplets is expanded to the well-known bench: the coalescence of the droplets in a T-junction. The continuous phase is injected by the two branches of the T-junction (Fig.1.11). Initially, two droplets are arranged symmetrically in the T-junction. Figs. 1.11 and 1.12 present their evolution into the micro channel.

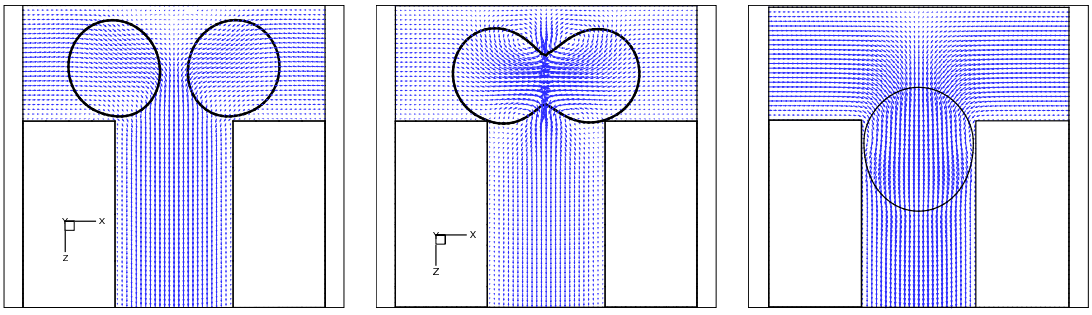

Fig. 1.11. Coalescence of two microdroplets in a T-junction (2D slices in the flow direction).

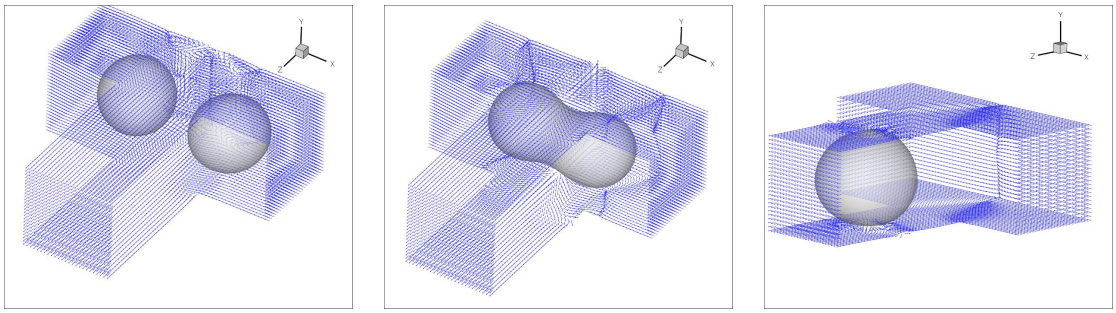

Fig. 1.12. Coalescence of two microdroplets in a T-junction (3D view).

1.5.3. *Parallel flows in a T-junction*

We are now interested in the location of the interface, at a junction between two fluids moving in parallel. The ratio of the viscosity is about 7.5 and the flow rates are identical. The interface moves into the channel according to their respective viscosity even if the computation does not reflect a realistic wetting condition on the top wall. The experimental set-up is used as a rheometer. Knowing one flow, the location of the interface allows to derive the viscosity of the other flow. Here, we want to quantify the impact of a defect on the surface of the channel on the location of this interface. On Fig.1.13 is represented the flow in presence of a defect. The difference between the two solid lines shows the impact of this defect on the location and consequently to the determination of the unknown viscosity which is not negligible. However this difference is significant only in the vicinity of the defect, elsewhere the interfaces are superimposed.

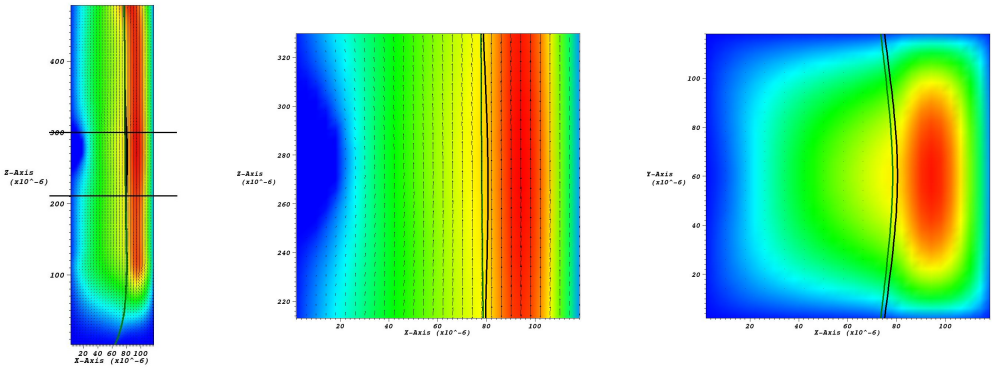

Fig. 1.13. Flows in the exit channel of the T-junction in presence of a defect on the surface of the channel. Global view (left), zoom around the defect in the x-z plane (middle) and in the x-y plane (right). The solid lines represent the interface without (left one) and with (right one) the defect.

1.5.4. *Performance and parallelization*

As it has been seen in the section dealing with the numerical stability, the stability condition is very restrictive in microfluidics. The computational times are extremely long. To get an idea, simulating a series of drops in a micro channel with eight hundred thousand unknowns takes about 720 hours. This computational time is given in the best case when the field is numbered locally. The same simulation with the global structure is drastically longer. Indeed, the approach has advantages in terms of the numerical implementation because once the code structure is set, it is easy to treat a variety of geometries. However, the main drawback is the need for indirect access machine that induces an increase of the computational time. In order to decrease this time, the code is parallelized using the libraries OpenMP. Therefore, the code sequence includes parallel regions for operations such Blas(1) and Blas(2). For the version of the code using the local numbering, the speed up obtained is around 2.5 with 4 threads, on 64 bits Opteron processors. Unfortunately, the performances are not improved on 8 threads. Moreover the parallelization with OpenMP is ineffective in the case where a global numbering is realized as the storage of the matrices is realized in the compressed row storage format. The works of Kotakemori et al.[13] on the subject show that there is a dependency between the storage format used for the matrices and the memory architecture of the machines.

1.6. Conclusion

The Level Set method proposed by Osher and Sethian is used in order to follow the interface between two flows such that their motion is mostly governed by the pressure gradient and the surface tension. This method gives results in good agreement with the experiments as the main quantities like the curvature and the unit normal are well computed. This study allows to analyze the breaking jet phenomenon and gives access to quantities like the pressure and the velocity of the droplet when it is created. A special care on the representation of the internal capillary employed as an injector allows to compare the volumes of the micro droplets for several radius of injectors. The influence of the capillaries of square section on the form of the created micro droplets is highlighted. In addition, the analysis of the internal dynamics of droplets show that playing on the physical parameters the shape of the droplets is changed as well as the areas of internal recirculations. Results concerning the coalescence of two micro droplets in a T-junction are proposed showing again that the Level Set method is perfectly suited to study these problems.

References

1. J.U. Brackbill, D.B. Kothe and C. Zemach, A Continuum Method for Modeling Surface Tension, *Journal of Computational Physics 100*, 1992.
2. C.-H. Bruneau and P. Fabrie, Effective downstream boundary conditions for incompressible Navier-Stokes equation, *Int.J. for Num. Methods in Fluids 19*, 1994.

3. C.-H. Bruneau and P. Fabrie, New efficient boundary conditions for incompressible Navier-Stokes equation: a well-posedness result, *M2AN 30*, 1996.
4. R. DeBar, Fundamentals of the KRAKEN Code, technical report UCIR-760, LLNL, 1974.
5. R. Eymard, T. Gallouet and R. Herbin, Finite Volume Methods. *Handbook of Numerical Analysis*, P.G Ciarlet, J.L Lions eds, 2007.
6. M. Fortin and R. Glowinski, Augmented lagrangian methods: applications to the numerical solution of boundary-value problems, *North-Holland Publishing Comp.(Studies in Mathematics and its Applications 15)*, 1983.
7. C. Galusinski and P. Vigneaux, Level-Set method and stability condition for curvature-driven flows, *C. R. Acad. Sci. Paris, Ser. I* **344**(11), 2007.
8. P. Guillot, P. Panizza, J.-B. Salmon, M. Joanicot, A. Colin, C.-H. Bruneau and T. Colin: Viscosimeter on a Microfluidic Chip, *Langmuir 22*, 2006.
9. P. Guillot, Ecoulement de fluides immiscibles dans un canal submillimétrique: Stabilité et application à la rhéologie, Thèse de Doctorat Université Bordeaux 1, 2006.
10. P. Guillot, A. Colin, A. Ajdari, Stability of a jet in confined pressure-driven biphasic flows at low Reynolds number in various geometries, Phys. Rev. E 78, 2008.
11. E. Guyon, J.P. Hulin and L. Petit, Hydrodynamique physique, EDP sciences/CNRS Editions, 2001.
12. G.S. Jiang and C.W Shu, Efficient Implementation of Weighted ENO Schemes. *Journal of Computational Physics 126*, 1996.
13. H. Kotakemori, H. Hasegawa and A. Nishida, Performance Evaluation of a Parallel Iterative Library using OpenMP. HPCASIA, 2005.
14. G-E. Karniadakis, and A. Beskok, Micro flows. Fundamentals and simulation. Springer Verlag, 2002.
15. S. Osher and J. Sethian, Fronts propagating with curvature-dependent speed: Algorithms based on the Hamilton-Jacobi formulation, *Journal of Computational Physics 79*, 1988.
16. S. Osher, R. Fedkiw, Level Set Methods and Dynamic Implicit Surfaces, *Applied Mathematical Sciences 153*. Springer
17. L. Rayleigh, On the Instability of Jets, Proc. Lond. Math. Soc. 10, 1879.
18. J. Li, Y. Renardy and M. Renardy, Numerical simulation of breakup of a viscous drop in simple shear flow through a volume-of-fluid method, *Physics of Fluids 19*, 2000.
19. F. Sarrazin, L. Prat, G. Casamatta, M. Joanicot, C. Gourdon et G. Cristobal, Microdrops approach in micro-reactors: mixing characterisation, *La Houille Blanche 3*, 2006.
20. J.A. Sethian, Level Set Methods and Fast Marching Methods - Evolving interfaces in computational geometry, fluid mechanics, computer vision and materials science, *Cambridge Monographs on Applied and Computational Mathematics*, 1999.
21. M. Sussman, P. Smereka and S. Osher, A level set approach for computing solutions to incompressible two-phase flow. *J. Comput. Phys 114*, 1994.
22. S. Tancogne, Calcul numérique et stabilité d'écoulements diphasiques tridimensionnels en microfluidique. Thèse de Doctorat Université Bordeaux 1, 2007.